

## On the Encounter Desorption of Hydrogen Atoms on Ice Mantle

Qiang Chang<sup>1</sup>, Xuli Zheng<sup>2</sup>, Xia Zhang<sup>2</sup>, Donghui Quan<sup>2,3</sup>, Yang Lu<sup>4</sup>, Qingkuan Meng<sup>1</sup>,  
 Xiaohu Li<sup>2</sup> and Long-Fei Chen<sup>2</sup>

<sup>1</sup> School of Physics and Optoelectronic Engineering, Shandong University of Technology, Zibo, 255000, China; [changqiang@sdut.edu.cn](mailto:changqiang@sdut.edu.cn)

<sup>2</sup> Xinjiang Astronomical Observatory, Chinese Academy of Sciences, 150 Science 1-Street, Urumqi 830011, PR China; [zhangx@xao.ac.cn](mailto:zhangx@xao.ac.cn)

<sup>3</sup> Department of Chemistry, Eastern Kentucky University, Richmond, KY 40475, USA

<sup>4</sup> School of Physics & Astronomy, Sun Yat-Sen University, Zhuhai 519082, China

Received 20xx month day; accepted 20xx month day

**Abstract** At low temperatures ( $\sim 10$  K), hydrogen atoms can diffuse quickly on grain ice mantles and frequently encounter hydrogen molecules, which cover a notable fraction of grain surface. The desorption energy of H atoms on H<sub>2</sub> substrates is much less than that on water ice. The H atom encounter desorption mechanism is adopted to study the enhanced desorption of H atoms on H<sub>2</sub> substrates. Using a small reaction network, we show that the steady-state surface H abundances predicted by the rate equation model that includes H atom encounter desorption agree reasonably well with the results from the more rigorous microscopic Monte Carlo method. For a full gas-grain model, H atom encounter desorption can reduce surface H abundances. Therefore, if a model adopts the encounter desorption of H atoms, it becomes more difficult for hydrogenation products such as methanol to form, but it is easier for C, O and N atoms to bond with each other on grain surfaces.

**Key words:** astrochemistry-ISM: abundances-ISM: molecules-ISM

### 1 INTRODUCTION

The grain ice mantle is observed to be mainly composed of water ice (Öberg et al. 2011), thus, the substrate for the grain-surface chemical reactions is usually assumed to be water ice only in the traditional astrochemical models (Hasegawa et al. 1992; Hasegawa & Herbst 1993; Garrod & Herbst 2006). However, this assumption may not be valid if the grain ice mantle is composed of other surface species on which the desorption energies of surface species differ significantly from these on water ice. For instance, the desorption energy of surface species on H<sub>2</sub> substrate is more than one order of magnitude lower than that on water ice (Cuppen & Herbst 2007). If we still assume the substrates are water ice only, hydrogen molecules may be depleted in the gas phase and are frozen on grains at low temperatures and high densities (Hincelin et al. 2015). However, to the best of our knowledge, the depletion of H<sub>2</sub> has never been reported. So, for better astrochemical modeling, there should be at least two kinds of substrates on grain surface, water and molecular hydrogen in a chemical model.

In order to consider the much lower desorption energy of surface species on molecular hydrogen in astrochemical models, Morata & Hasegawa (2013) made a crude approximation and assumed that the dust grains are completely covered by H<sub>2</sub> at 10 K. However, to the best of our knowledge, the validity

of this assumption has not been proved. Garrod & Pauly (2011) suggested another approach to solve the problem. They used the fractional coverage of surface  $H_2$  to adjust the desorption energies on water ice in their models. The adjusted desorption energies are named the effective binding energies. One major limitation of this approach is that an empirical modifying factor has to be used to calculate the effective binding energies.

It is straightforward to include both  $H_2$  and water ice substrates in the microscopic Monte Carlo (MC) models (Chang et al. 2005; Cuppen et al. 2017). This numerical approach keeps track of the trajectory of each surface species when it hops among binding sites. If a surface species hops into a site where there is one  $H_2$  molecule, the substrate for that surface species is  $H_2$  ice. Otherwise, the substrate is water ice. However, this numerical approach is computationally expensive when the surface temperatures are high ( $\geq 15$  K) because the hopping events of surface species consume most CPU time at high temperatures. Therefore, so far this approach can only be used to simulate the chemistry of cold sources such as the dark molecular clouds.

Recently, a new mechanism called the encounter desorption was suggested so that surface  $H_2$  abundances on heterogeneous grain surface can be calculated by the rate equation (RE) approach (Hincelin et al. 2015). This mechanism considers the desorption of hydrogen molecules when they encounter other surface  $H_2$  molecules. The implementation of this mechanism in astrochemical models is very convenient. Only one extra surface reaction  $gH_2 + gH_2 \rightarrow H_2 + gH_2$  has to be added into the chemical reaction network, where the letter g designates surface species. Moreover, the rate coefficient of the extra surface reaction has a simple analytical formula (Hincelin et al. 2015). The calculated surface  $H_2$  abundances by the rate equation approach from models including this reaction agree reasonably well with the results calculated by the microscopic MC method.

Hydrogen atoms can diffuse almost as fast as  $gH_2$  on grain surface, so they should encounter  $H_2$  frequently on grain surfaces if  $gH_2$  is abundant. The desorption energy of H atoms on  $gH_2$  substrates is about 45 K (Cuppen & Herbst 2007), so H atoms should sublime quickly when they encounter  $gH_2$  molecules just like molecular hydrogen. Because the surface chemistry is dominated by hydrogenation reactions when the grain temperature is around 10 K, grain surface chemistry is likely to be affected if the encounter desorption of H atoms is included in models.

In this work, we investigate how grain surface chemistry are affected by the encounter desorption of H atoms. The paper is organized as follows. In Section 2, we derive math formula for the rate coefficient of H atom encounter desorption on grain surface. In Section 3, we show that for a simple reaction network that include the encounter desorption of H atoms, the surface H abundances calculated by the rate equation approach agree reasonably well with those predicted by the microscopic MC approach. In Section 4, we simulate a full gas-grain reaction network that includes the encounter desorption of  $gH_2$  molecules and  $gH$  atoms and present the impacts of  $gH$  atoms encounter desorption on the surface chemistry in cold cores. In Section 5, we summarize our findings and draw the conclusions.

## 2 THE ENCOUNTER DESORPTION OF H SURFACE ATOMS

Following the  $gH_2$  encounter desorption mechanism, in order to include the  $gH$  encounter desorption mechanism in a chemical model, we can simply add an extra reaction,  $gH + gH_2 \rightarrow H + gH_2$ , to the chemical reaction network. Before deriving the rate coefficient for this reaction, we first review the encounter desorption mechanism of  $gH_2$  and derive the rate coefficient for the reaction  $gH_2 + gH_2 \rightarrow H_2 + gH_2$ .

Figure 1 shows the diffusion of  $gH_2$  on a heterogeneous ice mantle composed of water ice and  $H_2$ . We assume that the ice mantle is mainly composed of water ice, which agrees with observations toward cold sources (Öberg et al. 2011). When a hydrogen molecule hops from a water ice binding site to another site that is occupied by  $gH_2$  as shown in the figure,  $gH_2$  desorption competes with the hopping events of  $gH_2$ . The probability that  $gH_2$  desorbs is given by the following equation (Chang et al. 2005),

$$P_{H_2} = \frac{b_{H_2H_2}}{b_{H_2H_2} + k_{H_2H_2}}, \quad (1)$$

where  $b_{H_2H_2}$  and  $k_{H_2H_2}$  are the thermal desorption and hopping rates of gH<sub>2</sub> on gH<sub>2</sub> substrates respectively. The thermal desorption rate of gH<sub>2</sub> on gH<sub>2</sub> substrates is,  $b_{H_2H_2} = \nu \exp(-E_{D_{H_2H_2}}/T)$  while the hopping rate of gH<sub>2</sub> on gH<sub>2</sub> substrates is,  $k_{H_2H_2} = \nu \exp(-E_{b_{H_2H_2}}/T)$ , where  $E_{D_{H_2H_2}}$  and  $E_{b_{H_2H_2}}$  are desorption energy and diffusion barrier of gH<sub>2</sub> on gH<sub>2</sub> substrates. Assuming the number of binding sites occupied by gH<sub>2</sub> is much smaller than the total number of binding sites on the grain surface, the rate coefficient for two hydrogen molecules to encounter is given by,

$$r_{H_2H_2} = \frac{2k_{H_2H_2}O}{S}, \quad (2)$$

where  $k_{H_2H_2O}$  is the hopping rate of gH<sub>2</sub> on water ice while S is the total number of binding sites on the grain surface. Similarly,  $k_{H_2H_2O} = \nu \exp(-E_{b_{H_2H_2O}}/T)$ , where  $E_{b_{H_2H_2O}}$  is the diffusion barrier of gH<sub>2</sub> on water ice. Finally, we have the rate coefficient for the reaction  $gH_2 + gH_2 \rightarrow H_2 + gH_2$ , which has a simple analytical form,

$$r_{encH_2} = r_{H_2H_2}P_{H_2}. \quad (3)$$

Figure 1 also shows the diffusion of gH on grain ice mantle and the encounter of gH and gH<sub>2</sub>. The rate coefficient for the reaction  $gH + gH_2 \rightarrow H + gH_2$ ,  $r_{encHH_2}$  can be derived as the follows. First, the probability that a gH atom desorbs into the gas phase after it encounters a gH<sub>2</sub> molecule is,

$$P_{HH_2} = \frac{b_{HH_2}}{b_{HH_2} + k_{HH_2}}, \quad (4)$$

where  $b_{HH_2} = \nu \exp(-E_{D_{HH_2}}/T)$  and  $k_{HH_2} = \nu \exp(-E_{b_{HH_2}}/T)$  are the thermal desorption and hopping rates of gH on gH<sub>2</sub> substrates respectively. The two parameters  $E_{D_{HH_2}}$  and  $E_{b_{HH_2}}$  are the desorption energy and diffusion barrier of gH on gH<sub>2</sub> respectively. The gH and gH<sub>2</sub> encounter rate coefficient is,

$$r_{HH_2} = \frac{k_{H_2H_2O} + k_{HH_2O}}{S}, \quad (5)$$

where  $k_{HH_2O}$  is the hopping rate of gH on water ice, which is dependent on the diffusion barrier of gH on water ice,  $k_{HH_2O} = \nu \exp(-E_{b_{HH_2O}}/T)$ . There are two possible scenarios that hydrogen atoms encounter hydrogen molecules. Either a gH atom hops into a site already occupied by gH<sub>2</sub> or vice versa. The encounter desorption of gH only occurs in the first case. We will explain the reason in the next section, where the microscopic MC method will be briefly introduced. The probability for the first case to occur is,  $P = \frac{k_{HH_2O}}{k_{H_2H_2O} + k_{HH_2O}}$ . Finally we have,

$$\begin{aligned} r_{encHH_2} &= r_{HH_2}P_{HH_2} \\ &= \frac{k_{HH_2O}b_{HH_2}}{S(b_{HH_2} + k_{HH_2})} \end{aligned} \quad (6)$$

Here we only consider thermal desorption in the above derivation. If other desorption mechanism such as photodesorption is included in the models (Öberg et al. 2007), we can show that the rate coefficient for gH encounter desorption is,

$$r_{encHH_2} = \frac{k_{HH_2O}(\sum_i b_{iHH_2})}{S(\sum_i b_{iHH_2} + k_{HH_2})}, \quad (7)$$

where  $\sum_i b_{iHH_2}$  are the sum of the rates of all possible desorption mechanisms for gH on gH<sub>2</sub> substrates.

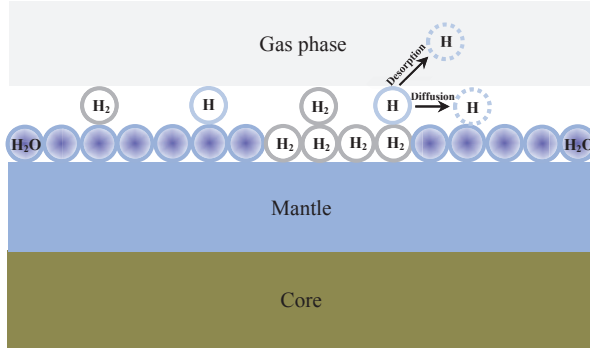


Fig. 1: The diffusion of  $\text{gH}_2$  and  $\text{gH}$  on substrates covered by water and  $\text{gH}_2$  and the encounter desorption of  $\text{gH}$ .

### 3 NUMERICAL COMPARISON

In order to test the validity of H atoms encounter desorption mechanism, we compare results from RE models with the inclusion of  $\text{gH}$  and  $\text{gH}_2$  encounter desorption mechanism (hereafter REED) with these calculated by the microscopic MC approach. However, so far it is not possible to simulate a chemical model that include  $\text{H}_2$  accretion for any meaningful length of time using the microscopic MC method because the  $\text{H}_2$  accretion and  $\text{gH}_2$  hopping consume too much CPU time. Therefore, following Hincelin et al. (2015), we can only compare the steady-state  $\text{gH}$  abundances calculated by these two approaches. Moreover, we also adopt a simple chemical model which only consider the accretion of H and  $\text{H}_2$ , the thermal and encounter desorption of  $\text{gH}$  and  $\text{gH}_2$  and the recombination of  $\text{gH}$  atoms on grain surfaces to form  $\text{gH}_2$ .

We adopt a typical dust grain with radius  $0.1 \mu\text{m}$ . A such grain has  $S = 10^6$  binding sites. The desorption energies of  $\text{gH}_2$  on water ice and  $\text{gH}_2$  are assumed to be 440 K (Hincelin et al. 2015) and 23 K (Cuppen & Herbst 2007) respectively while the desorption energy of  $\text{gH}$  on water ice and  $\text{gH}_2$  are assumed to be 450 K (Garrod & Herbst 2006) and 45 K (Cuppen & Herbst 2007) respectively. The diffusion barriers are always set to be half of the desorption energy for all surface species. Both the gas and dust temperatures are assumed to 10 K in our simulations. We assume the density of  $\text{H}_2$  to be constant in each simulation. We perform simulations using a wide range of H nuclei densities, which vary from  $2 \times 10^4 \text{ cm}^{-3}$  to  $2 \times 10^{14} \text{ cm}^{-3}$ . Because the fractional abundance of H is around  $1.0 \times 10^{-4}$  in dense clouds (Chang et al. 2007), we assume the fractional abundance of H atoms is fixed to be  $\frac{\sqrt{2}}{4} \times 10^{-4}$  for all H nuclei densities for simplicity. So, the accretion rate of H atom is,

$$k_{accH} X(H) = 1.0 \times 10^{-4} k_{accH_2} X(H_2), \quad (8)$$

where  $k_{accH_2}$  and  $k_{accH}$  are the accretion rate coefficients of gas-phase  $\text{H}_2$  and H respectively while  $X(\text{H}_2)$  and  $X(\text{H})$  are the densities of these two species respectively. Moreover, in order for a preliminary study of the effect of the  $\text{gH}$  encounter desorption on the surface chemistry, we also use the RE approach to calculate another chemical model which has all the above reactions other than the encounter desorption of  $\text{gH}$  atoms. Hereafter, this model is called REED2 model.

We briefly introduce the microscopic MC approach as the follows and refer to Chang et al. (2005) for details of this numerical method. Grain surface binding sites form a  $L \times L$  square lattice, where  $L = \sqrt{S}$ . When gas-phase species accrete on grains, they are randomly located into binding sites. At time  $t$ , a surface species  $\text{gI}$  either hop to a neighboring site or desorb after a waiting time,

$$\delta t = -\ln(X)/(b_I(t) + k_I(t)), \quad (9)$$

where  $b_I(t)$  and  $k_I(t)$  are the desorption and hopping rates of species I at the time  $t$  respectively while  $X$  is random number uniformly distributed within  $(0, 1)$ . If the site where species I resides at the time  $t$  is already occupied by  $\text{gH}_2$ , the value of  $b_I(t)$  should be the desorption rate of the species I on  $\text{gH}_2$ . Otherwise, it is the desorption rate of species I on water ice. Similarly, the value of  $k_I(t)$  depends on whether the binding site is occupied by  $\text{gH}_2$  or not. The species I hops into a neighboring site if  $k_I(t) \geq Y(b_I(t) + k_I(t))$ , where  $Y$  is another random number uniformly distributed within  $(0, 1)$ . Otherwise it will desorb. A chemical reaction occurs if the species I hops into a site and encounters a reactive species.

In the microscopic MC simulations, the initial  $\text{gH}$  and  $\text{gH}_2$  abundances are zero. As  $\text{H}$  and  $\text{H}_2$  accrete on the grain surface,  $\text{gH}$  abundance initially increases and then fluctuates around its mean value after the steady-state has been reached. The average abundance of  $\text{gH}$  between time  $t_0$  and  $t_1$ , which are both after the steady-state has been reached, is,

$$g\bar{H}(t_0, t_1) = \frac{\sum_i i \Delta t_i}{t_1 - t_0}, \quad (10)$$

where  $\Delta t_i$  is the time interval during which the number of  $\text{gH}$  atoms is  $i$  and  $\sum_i \Delta t_i = t_1 - t_0$ . If  $t_1 - t_0$  is sufficiently large,  $g\bar{H}$  converges to a value that is independent on  $t_1$ ,  $t_0$  nor  $t_1 - t_0$ . At the low  $\text{H}$  nuclei density ( $\sim 10^{-6} \text{ cm}^{-3}$ ),  $t_1 - t_0$  is a time period during which about 4000  $\text{H}$  atoms accrete on grain surface so that  $g\bar{H}$  can converge. As the  $\text{H}$  nuclei densities increase, more  $\text{H}$  atoms are required to accrete during the time period  $t_1 - t_0$  so that  $g\bar{H}$  converges because of the larger  $\text{gH}$  population fluctuations. We use the converged  $g\bar{H}$  values to compare with the abundances of  $\text{gH}$  predicted by RE approach.

As introduced earlier, hydrogen atoms can encounter  $\text{gH}_2$  in two different ways. When a  $\text{gH}$  atom hops into a site occupied by  $\text{gH}_2$ , the desorption and hopping rates of  $\text{gH}$  significantly increase because of the significantly reduced desorption energy and diffusion barrier of  $\text{gH}$  on  $\text{gH}_2$ . On the other hand, when a  $\text{gH}_2$  molecule hops into a water binding site occupied by a  $\text{gH}$  atom, the  $\text{gH}$  atom cannot hop or desorb until the  $\text{gH}_2$  molecule leaves the binding site in the microscopic MC simulations (Chang et al. 2007). After the  $\text{gH}_2$  leaves the binding site, the  $\text{gH}$  atom can hop or desorb, but its desorption energy and diffusion barrier are still these on water substrates. Therefore, the first scenario of  $\text{gH}_2$  and  $\text{gH}$  encounter must occur so that  $\text{gH}$  desorb more quickly. If the second scenario occurs,  $\text{gH}_2$  may also desorb more quickly on that site than on water ice because the desorption energy of  $\text{gH}_2$  on  $\text{gH}$  is much less than that on water ice (Cuppen & Herbst 2007). A surface reaction  $\text{gH} + \text{gH}_2 \rightarrow \text{gH} + \text{H}_2$  can be included in the reaction network in the RE approach in order to take into account of this  $\text{gH}_2$  molecules desorption process when they encounter  $\text{gH}$  atoms. However, because  $\text{gH}_2$  is much more abundant than  $\text{gH}$ , this event occurs much less frequently than the process  $\text{gH}_2$  encounter other hydrogen molecules does. Therefore, in this work, we ignore this desorption process and assume that the desorption energy of  $\text{gH}_2$  on  $\text{gH}$  is the same as that on water ice. Thus, the reaction  $\text{gH} + \text{gH}_2 \rightarrow \text{gH} + \text{H}_2$  is not included in the reaction network.

Figure 2 shows the steady-state  $\text{gH}$  abundance as a function of  $\text{H}_2$  density from the microscopic MC and REED models. It can be seen that the  $\text{gH}$  abundances predicted by the REED models agree very well with the results from the microscopic MC model for a wide range of  $\text{H}_2$  density between  $10^4 \text{ cm}^{-3}$  and  $10^{12} \text{ cm}^{-3}$ . At the density of  $10^4 \text{ cm}^{-3}$ ,  $\text{gH}$  abundance predicted by the microscopic MC method is slightly higher than that from the REED model because of the “back diffusion” problem. When the abundances of reactive surface species are very low on grain surface, two species must visit around 3S binding sites in order to encounter each other (Lohmar & Krug 2006; Chang et al. 2006). So the reaction rates in the RE model are over estimated while the microscopic MC method already takes into account the back diffusion. At higher  $\text{H}_2$  densities, surface  $\text{H}_2$  density also increases so that the back diffusion problem becomes less significant (Chang et al. 2006). Thus, the REED model results agree better with the microscopic MC model results. However when the  $\text{H}_2$  density is above  $10^{13} \text{ cm}^{-3}$ , the microscopic MC model predicts that hydrogen molecules occupy about 70 percent of the total number of grain surface binding sites (Hincelin et al. 2015). If  $\text{gH}$  hops from one binding site to another, it is very likely that the second binding site is also occupied by  $\text{gH}_2$ . This possibility is not considered by the

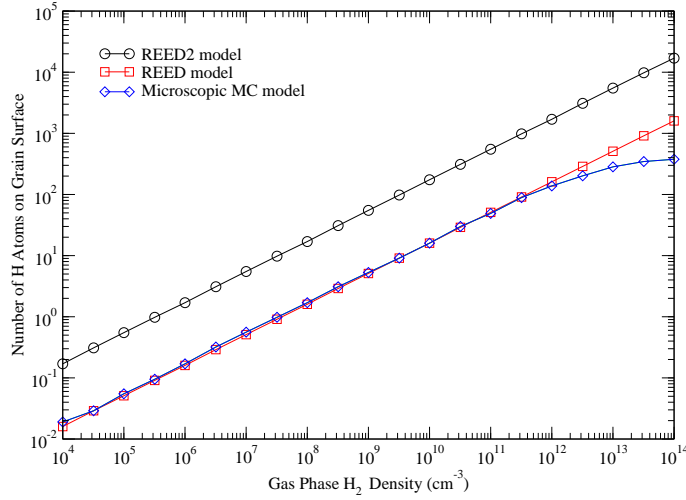


Fig. 2: The steady-state surface H atom abundances with respect to  $H_2$  density predicted by the REED, REED2 and microscopic MC models using a simple chemical reaction network.

RE approach. Therefore, the discrepancy between the REED and microscopic model results increase as gas-phase  $H_2$  abundance increases. At the highest  $H_2$  density, the abundance of gH from the REED model is about a factor of four larger than that from the microscopic MC model.

Figure 2 also shows the steady-state gH abundance as a function of  $H_2$  density for the REED2 model. We can see that the gH encounter desorption mechanism can decrease gH abundance by about one order of magnitude for the simple reaction network. Grain surface reactions are dominated by hydrogenation reactions at 10 K, so the significant decrease of gH abundance may change the abundances of icy species in a much larger gas-grain chemical model. The effects of gH encounter desorption on the formation of surface species at 10 K in a larger chemical model will be presented in the next section.

We fix the fractional abundance of H atoms to be  $\frac{\sqrt{2}}{4} \times 10^{-4}$  in the above simulations, however, the fractional abundances of H atoms in astronomical sources may not be always around that value. In order to study how the fractional abundances of H may affect the validity of H atoms encounter desorption mechanism, we fix the H nuclei density to be  $2 \times 10^6 \text{ cm}^{-3}$  and simulate the REED and microscopic MC models using a wide range of H fractional abundances, which vary from  $10^{-6}$  to 0.1. We found that the gH abundances predicted by the REED model fall within 50 percent of that by the microscopic MC model over the wide range of H fractional abundances. Therefore, the agreement of the REED model with the microscopic MC model results is not likely to be noticeably affected by the fractional abundance of H atoms.

#### 4 EFFECTS OF H ATOMS ENCOUNTER DESORPTION ON THE COLD CORE CHEMISTRY

The encounter desorption mechanism is not likely to be important when grain temperatures are high enough so that almost all  $gH_2$  molecules sublime because the encounter events would be few if  $gH_2$  abundance is low. Therefore, we only study the effects of H atoms encounter desorption on cold core chemistry.

The full gas-grain chemical reaction network was adapted from Garrod et al. (2007) and updated based on KIDA (Hincelin et al. 2011), which has 654 species and 6210 chemical reactions. The reactive desorption mechanism is included in this reaction network. Its coefficient is set to be 0.01. Initially, all species are assumed to be in the gas phase. The initial low-metal elemental abundances are taken from Semenov et al. (2010). The effect of quantum tunneling for grain-surface species is not considered in this work (Katz et al. 1999). The two-phase model is used in all simulations. We use a standard dust



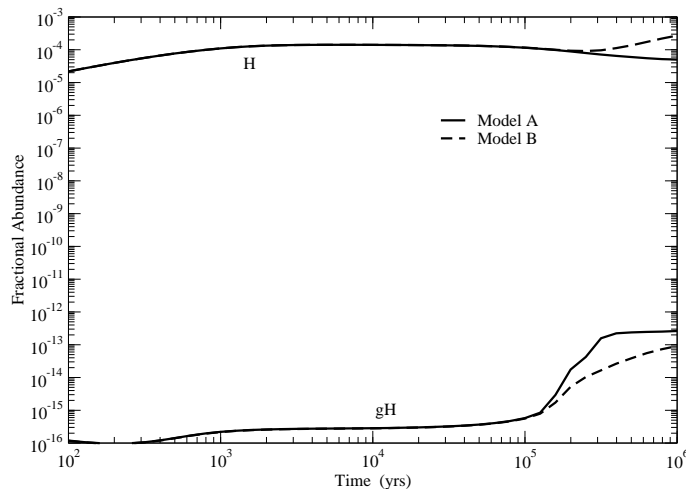


Fig. 3: The gas-phase and surface H atom abundances as a function of time in models A and B.

grain with radius  $0.1 \mu\text{m}$  with surface binding site density  $1.5 \times 10^{15} \text{ cm}^{-2}$ . Both the grain and gas phase temperatures are set to 10 K and the density of H nuclei is  $2 \times 10^4 \text{ cm}^3$  in our models. The cosmic-ray ionization rate is  $1.3 \times 10^{-17} \text{ s}^{-1}$  and the visual extinction is 10 mag. Similar to the simple reaction network discussed above, the desorption energies of gH on water ice and gH<sub>2</sub> are 450 K and 45 K respectively while the desorption energies of gH<sub>2</sub> on water ice and gH<sub>2</sub> are 440 and 23 K respectively. The ratio of the diffusion barrier of each surface species to its desorption energy is kept to be 0.5 in our models.

We simulate two chemical models. Model A includes the reaction  $\text{gH}_2 + \text{gH}_2 \rightarrow \text{H}_2 + \text{gH}_2$  but not the reaction  $\text{gH} + \text{gH}_2 \rightarrow \text{H} + \text{gH}_2$ . In model B, the two reactions  $\text{gH}_2 + \text{gH}_2 \rightarrow \text{H}_2 + \text{gH}_2$  and  $\text{gH} + \text{gH}_2 \rightarrow \text{H} + \text{gH}_2$  are included in its reaction network. In total, there are 6211 and 6212 chemical reactions in models A and B respectively. Both models are calculated by the OSU gas-grain rate equation codes (Garrod & Herbst 2006).

Figure 3 shows the temporal evolution of gas-phase and surface H atom abundances predicted by models A and B. Because the H atom encounter desorption mechanism is included in model B, gH abundance from model B is typically lower than from model A. It is interesting that at the time earlier than  $10^5$  yrs, models A and B predict similar gH and H abundances, which can be explained as the follows. At the early time, there are abundant O, C and N in the gas phase, so most gH atoms react with gO, gC and gN on grain surface instead of encountering gH<sub>2</sub> molecules and desorbing. When O, C and N atoms are depleted in the gas phase, it becomes more difficult for gH to find these atoms on grain surface to recombine, so gH can encounter gH<sub>2</sub> molecules more frequently. As a result, the impact of gH encounter desorption becomes more significant. Thus, the discrepancy between the gH abundances predicted by these two models becomes larger. At the time later than  $3 \times 10^5$  yrs, however, gH abundances predicted by model B become closer to that by model A, which can be explained as the follows. In Figure 3, after  $3 \times 10^5$  yrs, the gas-phase H atom abundances gradually increase with time in model B while its abundances decrease with time in model A. At the time  $10^6$  yrs, gas-phase H atom abundance in model B is about a factor of 4 larger than that in model A. Because of the higher gas-phase H atom density in model B, more H atoms accrete on grains in model B than in model A after the time  $3 \times 10^5$  yrs. So, gH abundances in model B are closer to that in model A after the time  $3 \times 10^5$  yrs. The largest discrepancy between the gH abundances predicted by these two models is about one order of magnitude, which occurs at around the time  $3 \times 10^5$  yrs.

Figure 4 shows selected major surface species abundances as a function of time from models A and B. These species are all surface hydrogenated products. We can see that the production of water ice and gNH<sub>3</sub> are not much affected by the gH encounter desorption mechanism introduced in model

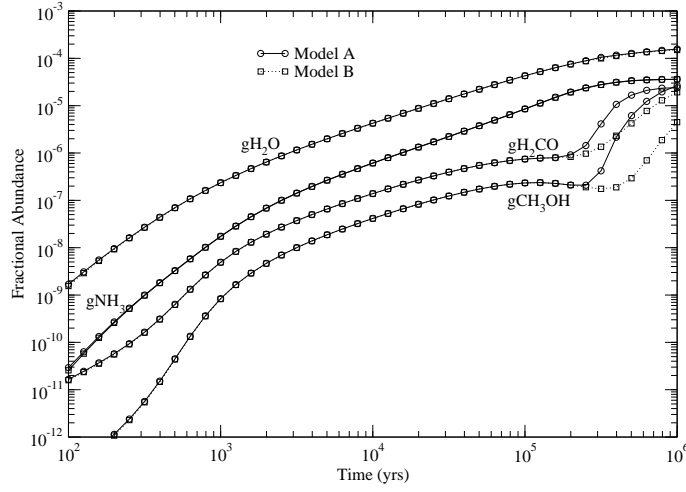


Fig. 4: The fractional abundances of selected major icy species as a function of time in models A and B.

B. However, after the time  $10^5$  yrs, model B predicts lower  $\text{gCH}_3\text{OH}$  and  $\text{gH}_2\text{CO}$  abundances than model A does because  $\text{gH}$  atom abundances in model B are lower. Difference of the impact on surface species production may be explained by the reaction barriers of hydrogenation reactions. Hydrogenation reactions that form  $\text{gH}_2$  and  $\text{gNH}_3$  are barrierless, thus, the rate coefficients of these hydrogenation reactions are large enough so that even when the  $\text{gH}$  abundances decrease, almost all  $\text{gO}$  and  $\text{gN}$  atoms can still be hydrogenated to form water and  $\text{gNH}_3$  respectively. On the other hand, not all  $\text{gCO}$  molecules can be hydrogenated because the hydrogenation reaction  $\text{gH} + \text{gCO} \rightarrow \text{gHCO}$  has a barrier. So, when the encounter desorption is introduced in model B, less  $\text{gCO}$  can be hydrogenated, thus, less  $\text{gCH}_3\text{OH}$  and  $\text{gH}_2\text{CO}$  molecules are formed in model B. We can also see that although it is more difficult to hydrogenate  $\text{gH}_2\text{CO}$  to form  $\text{gCH}_3\text{OH}$  in model B, overall, the  $\text{gH}_2\text{CO}$  abundances are reduced by the  $\text{gH}$  encounter desorption mechanism. The abundance of another major surface species  $\text{gCO}$  in models A and B differ by a factor less than 3. The abundances of  $\text{gCO}$  predicted by model B is always higher than that by model A after the time  $10^5$  yrs because it is easier to hydrogenate  $\text{gCO}$  in model A due to the higher  $\text{gH}$  atom abundances.

The abundances of minor surface species may be more strongly affected by the encounter desorption of  $\text{gH}$ . Figure 5 shows the temporal evolution of selected minor surface species abundances from models A and B. After  $10^5$  yrs, the abundances of these surface species from model B can be more than one order of magnitude higher than the results from model A. The encounter desorption of  $\text{gH}$  reduces its abundance in model B, so it is more likely that  $\text{gO}$ ,  $\text{gN}$  and  $\text{gC}$  atoms react with each other to form  $-\text{O}-\text{O}-$ ,  $-\text{C}-\text{C}-$  or  $-\text{C}-\text{N}-$  chemical bonds instead of reacting with  $\text{gH}$  atoms in this model. Thus, more  $\text{gH}_2\text{O}_2$ ,  $\text{gO}_3$ , and  $\text{gHC}_3\text{N}$  can be formed in this model than in model A.

The encounter desorption of  $\text{gH}$  may also impact the abundances of gas-phase species. Figure 6 shows the temporal evolution of selected gaseous species abundances. If a gas-phase species is mainly produced in the gas phase, the  $\text{gH}$  encounter desorption is unlikely to impact its abundance. For instance,  $\text{HC}_3\text{N}$  is mainly synthesized in gas phase, so its abundances predicted by models A and B are almost the same. On the other hand, methanol can hardly be produced in the gas-phase. Almost all gaseous methanol are formed via reactive desorption on grain surface. Therefore,  $\text{CH}_3\text{OH}$  abundance from model B is much lower than those from model A after the time  $10^5$  yrs because surface methanol can be more efficiently synthesized in model A. Both  $\text{H}_2\text{O}_2$  and  $\text{H}_2\text{CO}$  can be formed in the gas phase and via reaction desorption on grain surfaces. So, the impact of the  $\text{gH}$  encounter desorption on their abundances is less than that on methanol abundances, but more than that on  $\text{HC}_3\text{N}$  abundances.

We also performed test simulations of the above two models at a higher H nuclei density,  $10^5 \text{ cm}^{-3}$ . Similarly, model B considers the  $\text{gH}$  atom encounter desorption mechanism while model A does not.



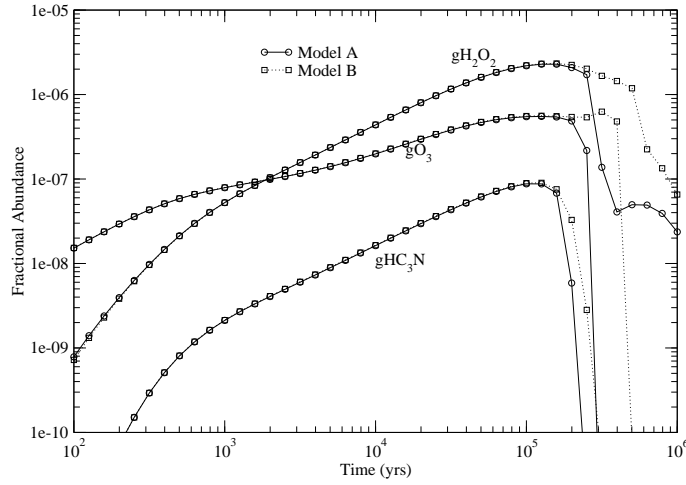


Fig. 5: The temporal evolution of the fractional abundances of selected minor icy species in models A and B.

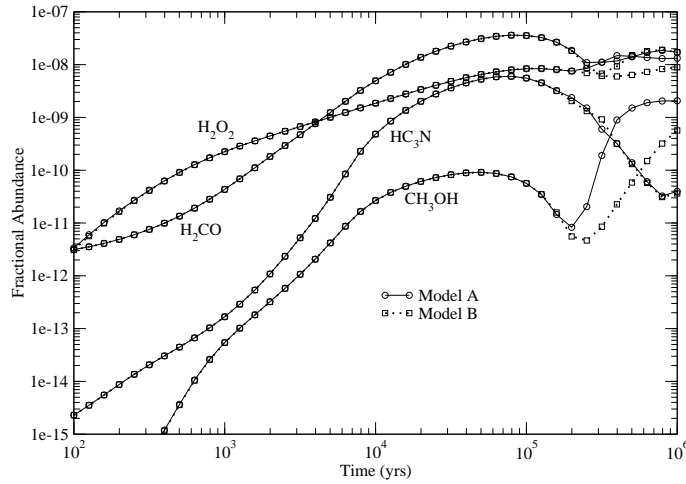


Fig. 6: The fractional abundances of selected gas-phase species as a function of time in models A and B.

We found that there are also less  $\text{gCH}_3\text{OH}$  and  $\text{gH}_2\text{CO}$  molecules and more surface species such as  $\text{gO}_3$  in model B at the higher density. On the other hand, discrepancy between species abundances in the two models becomes less significant at the higher H nuclei density. For instance, the surface methanol abundances from the model B are no more than a factor of 5 lower than that from model A at the higher H nuclei density while the discrepancy can be as much as one order of magnitude at the lower H nuclei density. We explain the decrease of the impact of the gH encounter desorption when the H nuclei density increases as the follows. At the higher H nuclei density, more species that can react with gH accrete on grain surfaces, so it is more likely that gH atoms react with other surface species instead of desorbing. So, the gH encounter desorption mechanism affects grain surface chemistry less significantly at the higher H nuclei densities.

## 5 CONCLUSIONS AND DISCUSSIONS

The significantly reduced desorption energy of hydrogen atoms when encountering hydrogen molecules on dust grains, namely the encounter desorption mechanism of hydrogen atoms, is investigated in this work. This process can be easily included in an astrochemical model by adding a new chemical reaction,  $\text{gH} + \text{gH}_2 \rightarrow \text{H} + \text{gH}_2$  to the chemical reaction network. We derived the rate coefficient for this reaction. In order to test the validity of hydrogen atom encounter desorption mechanism, we simulated a simple chemical reaction network that includes the encounter desorption of H atoms by the RE approach and calculated the steady-state surface H atom abundances. The calculated H atom abundances agree well with those predicted by the more rigorous microscopic MC method over a wide range of gas phase  $\text{H}_2$  and H densities. Thus, the hydrogen atom encounter desorption mechanism is a reasonable approach to take into account of the facile desorption of hydrogen atoms on substrates composed of hydrogen molecules and water ice.

We simulated two full gas-grain chemical models under standard physical conditions that pertain to dense cores to investigate the impact of gH encounter desorption mechanism. The gH encounter desorption mechanism is present in model B, but not in model A. We found that the gH atom encounter desorption can affect grain surface chemistry in two ways. Firstly, it becomes more difficult for hydrogenation reactions with barriers to fire if the gH atom encounter desorption mechanism is included in the chemical model. Thus, the abundances of surface species such as methanol drops in the model because surface reactions that produce these surface species have barriers. Secondly, gO, gN and gC atoms are more likely to react with each other instead of reacting with gH atoms in a model that includes the gH atom encounter desorption mechanism.

Our approach can be generalized to other cases in which the facile desorption of a surface species gX on a substrate gY other than water ice has to be considered. We can simply add one surface reaction,  $\text{gX} + \text{gY} \rightarrow \text{X} + \text{gY}$  in the chemical reaction network. The rate coefficient for this reaction can be derived in the same way as that for gH encounter desorption.

Initially, the  $\text{gH}_2$  encounter desorption mechanism was suggested to solve the problem that the coverage of  $\text{gH}_2$  is too high at low temperatures and high H nuclei densities. Our study shows that at the lower H nuclei density, the gH encounter desorption mechanism may affect the production of surface species significantly. On the other hand, the major advantage of this approach is that it is very simple and easy to be implemented in a chemical model. Thus, this mechanism could be adopted widely in astrochemical modeling.

**Acknowledgements** We thank our referee for his/her constructive comments to improve the quality of the manuscript. The research was funded by The National Natural Science Foundation of China under grant 11673054, 11973075 and 11973099.

## References

- Chang, Q., Cuppen, H. M., & Herbst, E. 2005, *A&A*, 434, 599 [2](#), [4](#)
- Chang, Q., Cuppen, H. M., & Herbst, E. 2006, *A&A*, 458, 497 [5](#)
- Chang, Q., Cuppen, H. M., & Herbst, E. 2007, *A&A*, 469, 973 [4](#), [5](#)
- Cuppen, H. M., & Herbst, E. 2007, *ApJ*, 668, 294 [1](#), [2](#), [4](#), [5](#)
- Cuppen, H. M., Walsh, C., Lamberts, T., et al. 2017, *Space Sci. Rev.*, 212, 1 [2](#)
- Garrod, R. T., & Herbst, E. 2006, *A&A*, 457, 927 [1](#), [4](#), [7](#)
- Garrod, R. T., & Pauly, T. 2011, *ApJ*, 735, 15 [2](#)
- Garrod, R. T., Wakelam, V., & Herbst, E. 2007, *A&A*, 467, 1103 [6](#)
- Hasegawa, T. I., & Herbst, E. 1993, *MNRAS*, 261, 83 [1](#)
- Hasegawa, T. I., Herbst, E., & Leung, C. M. 1992, *ApJS*, 82, 167 [1](#)
- Hincelin, U., Chang, Q., & Herbst, E. 2015, *A&A*, 574, A24 [1](#), [2](#), [4](#), [5](#)
- Hincelin, U., Wakelam, V., Hersant, F., et al. 2011, *A&A*, 530, A61 [6](#)
- Katz, N., Furman, I., Biham, O., Pirronello, V., & Vidali, G. 1999, *ApJ*, 522, 305 [6](#)
- Lohmar, I., & Krug, J. 2006, *MNRAS*, 370, 1025 [5](#)

- Morata, O., & Hasegawa, T. I. 2013, MNRAS, 429, 3578 [1](#)
- Öberg, K. I., Boogert, A. C. A., Pontoppidan, K. M., et al. 2011, ApJ, 740, 109 [1](#), [2](#)
- Öberg, K. I., Fuchs, G. W., Awad, Z., et al. 2007, ApJ, 662, L23 [3](#)
- Semenov, D., Hersant, F., Wakelam, V., et al. 2010, A&A, 522, A42 [6](#)